**Summary**
Accuracy of depth seismic imaging depends on the accuracy of the velocity models used for wavefield reconstruction. Models can be decomposed in two components corresponding to large scale and small scale variations. In practice, the large scale velocity model component can be estimated accurately, but the small scale component cannot. Therefore, wavefield reconstruction does not completely describe the recorded data and migrated images are perturbed by artifacts.

There are two ways to address this problem: improve wavefield reconstruction by estimating more accurate velocity models and image using conventional techniques, or reconstruct wavefields with conventional methods using the known smooth velocity, and improve the imaging condition to alleviate the artifacts caused by the imprecise reconstruction.

The unknown component of the velocity model can be described as a random function with local spatial correlations. Imaging data perturbed by such random variations is characterized by statistical instability, i.e. various wavefield components image at wrong locations that depend on the actual realization of the random model. Statistical stability can be achieved by local wavefield averaging either in spatial windows defined in the vicinity of the data acquisition locations, or in local windows defined in the vicinity of image points.

**Seismic imaging theory**
Conventional seismic imaging methods share the fundamental assumption of single scattering in the subsurface (Born approximation). Under this assumption, we can represent waves recorded at the surface as a convolution of Green's functions ($G$) corresponding to sources on the surface and scattering points in the subsurface. Assuming an impulsive source, we can write

$$P(\mathbf{x}_m, \omega_m) = G(\mathbf{x}_s, \mathbf{y}_m, \omega_m)\, G(\mathbf{y}_m, \mathbf{x}_m, \omega_m) \ , \tag{1}$$

where $P$ denotes recorded acoustic data at coordinates $\mathbf{x}_m$, $\mathbf{x}_s$ are coordinates of the source, $\mathbf{y}_m$ are coordinates of the scattering points, and $\omega_m$ is the frequency of the propagating wave. The Green's function $G$ characterizes data propagation in the real medium of velocity $v$.

Imaging with recorded data $P(\mathbf{x}_m, \omega_m)$ is a two-step procedure: the first step consists of extrapolation of a source wavefield forward in time, and extrapolation of the recorded wavefield backward in time; the second step consists of an imaging condition evaluating whether the two extrapolated wavefields match kinematically, which indicates if a reflector is present in the medium.

A conventional imaging condition (CIC) involves cross-correlation of the source and receiver wavefields (Claerbout, 1985). Thus, the image $R$ is evaluated using the relation

$$R(\mathbf{y}_m) = \int_{\omega_m} d\omega_m \int_{\mathbf{x}_m} d\mathbf{x}_m \, \overline{G_0(\mathbf{x}_s, \mathbf{y}_m, \omega_m)} P(\mathbf{x}_m, \omega_m) \, \overline{G_0(\mathbf{y}_m, \mathbf{x}_m, \omega_m)} \ . \tag{2}$$

Maximum energy at zero temporal cross-correlation lag, computed by summation over temporal frequency, indicates the presence of reflectors.

The assumption made in this model is that Green's functions used for reconstruction are accurate representations of Green's functions describing wave propagation in the real medium. However, for the case of media with random velocity fluctuations, $v_0$ is a homogenized velocity approximating $v$. Although the general kinematics of wave propagation are accurately described by $v_0$, the velocity fluctuations induce perturbations of the wavefield leading to imaging artifacts.

**Coherent interferometry**

One way of addressing the problem of imaging in models with random fluctuations involves statistical stabilization using phase compensation in windows localized in time and space (Papanicolaou et al., 2004; Fouque et al., 2005). The idea is that small wavefield fluctuations caused by random perturbations of the velocity model are incoherent spatially and temporally and cancel-out by local cross-correlation and averaging.

Borcea et al. (2006) exploit the idea of achieving statistical stability for imaging in random media by developing the *coherent interferometric imaging* technique. Interferometric imaging methods are capable of reducing imaging artifacts and statistically stabilizing the image by averaging locally in space and time (or frequency) the fluctuations caused by the random variations of the medium. The modified imaging functional is

$$R(\mathbf{y}_m) = \int_{\omega_m} d\omega_m \int_{\mathbf{x}_m} d\mathbf{x}_m \, \overline{G_0(\mathbf{x}_s, \mathbf{y}_m, \omega_m)} \left[ \int_{\mathbf{x}_h} d\mathbf{x}_h \int_{\omega_h} d\omega_h P(\mathbf{x}_m - \mathbf{x}_h, \omega_m - \omega_h) \, \overline{P(\mathbf{x}_m + \mathbf{x}_h, \omega_m + \omega_h)} \right] \overline{G_0(\mathbf{y}_m, \mathbf{x}_m, \omega_m)} \,, \quad (3)$$

where $\omega_h$ represents the frequency integration variable in a frequency window $\Omega$ (decoherence frequency), and $\mathbf{x}_h$ is a space integration variable in a space window $X$ (decoherence length) defined around a receiver location on the acquisition surface.

**Interferometric imaging condition**

An alternative approach to the coherent imaging problem is to reconstruct wavefields at all locations in the imaging volume from recorded data and attenuate the random fluctuations in the wavefield by local cross-correlations in small windows around the image point. In this case, we can define another decoherence length around an image point $Y$, which is analogous to the decoherence length defined on the acquisition surface $X$. The imaging functional is

$$R(\mathbf{y}_m) = \int_{\omega_m} d\omega_m \int_{\mathbf{x}_m} d\mathbf{x}_m \, \overline{G_0(\mathbf{x}_s, \mathbf{y}_m, \omega_m)} \int_{\mathbf{y}_h} d\mathbf{y}_h \left[ P(\mathbf{x}_m, \omega_m) \, \overline{G_0(\mathbf{y}_m - \mathbf{y}_h, \mathbf{x}_m, \omega_m)} \right] \overline{\left[ P(\mathbf{x}_m, \omega_m) \, \overline{G_0(\mathbf{y}_m + \mathbf{y}_h, \mathbf{x}_m, \omega_m)} \right]} \,. \quad (4)$$

The imaging procedure described by equation (4) exploits two ideas: The first idea is that of extended imaging conditions (Rickett and Sava, 2002; Sava and Fomel, 2006) where space and time lags of the wavefield cross-correlation are evaluated. In particular, $\mathbf{y}_h$ is interpreted as the 3D spatial lag of the cross-correlation. This lag can be used for decomposition of migrated images function of scattering angles (Sava and Fomel, 2003; Biondi and Symes, 2004). Here, we use $\mathbf{y}_h$ as a summation variable during averaging around image locations. The second idea is that statistical stability in random media is achieved by space and time averaging of wavefield cross-correlations in local windows (Papanicolaou et al., 2004; Fouque et al., 2005). We exploit this idea similarly to Borcea et al. (2006) for coherent interferometric imaging in clutter. The local averaging variable $\mathbf{y}_h$ is similar to the local averaging variable $\mathbf{x}_h$, but $\mathbf{y}_h$ is defined in the image space, around particular image points. Unlike $\mathbf{x}_h$ which is a 2D quantity defined on the acquisition surface, $\mathbf{y}_h$ is a 3D quantity defined in a volume around the image locations. Unlike $\mathbf{x}_h$ which requires close spacing on the acquisition surface, $\mathbf{y}_h$ is defined around image locations and does not require special sampling assumptions.

We can name the imaging method summarized by equation (4) *interferometric imaging condition* (IIC), since it acts similarly to CIC, but ads robustness with respect to random fluctuations due to local interferometric averaging around image locations.

**Example**

We demonstrate the interferometric imaging condition applied to complex stratigraphy in a medium with random velocity variations. Accurate imaging in this situation requires velocity models incorporating all random velocity variations. However, practical migration velocity analysis approximates models them with smooth fluctuations one order of magnitude larger than the typical seismic wavelength. This situation is simulated using the models in figures 1(a)-1(b). The imaging target is represented by the lines located around $z = 700$ m, representing a cross-section of a complex stratigraphic model. Data are simulated in the two respective models, but imaging is done using the smooth model from figure 1(a). figures 1(a)-1(b) show wavefield snapshots in the two models, and figures 1(c) and 1(d) show the corresponding recorded data.

Data migrated using CIC equation (2) are shown in figures 1(e) and 1(f), corresponding to data from figures 1(c) and 1(d), respectively. Modeling and migration in the smooth model produce the image in figure 1(e). The targets are well imaged, although the image also shows artifacts due to truncation of the data on the acquisition surface. In contrast, migration with the conventional imaging condition of data simulated in the random model using the smooth velocity produces the image in figure 1(f) showing many imaging artifacts due to incorrect velocity.

Data migrated using IIC equation (4) are shown in figures 1(g) and 1(h). Artifacts caused by the inaccurate velocity model are attenuated and the imaging targets are more clearly visible and easier to interpret. Furthermore, the general patterns of amplitude variation along the imaged reflectors are similar between figures 1(f) and 1(h).

**Acknowledgments**
Paul Sava acknowledges the financial support of the sponsors of the Center for Wave Phenomena at Colorado School of Mines.

## REFERENCES

Biondi, B. and W. W. Symes, 2004, Angle-domain common-image gathers for migration velocity analysis by wavefield-continuation imaging: Geophysics, **69**, 1283–1298.

Borcea, L., G. Papanicolaou, and C. Tsogka, 2006, Coherent interferometric imaging in clutter: Geopysics, **71**, SI165–SI175.

Claerbout, J. F., 1985, Imaging the Earth's interior: Blackwell Scientific Publications.

Fouque, J., J. Garnier, A. Nachbin, and K. Solna, 2005, Time reversal refocusing for point source in randomly layered media: Wave Motion, **42**, 191–288.

Papanicolaou, G., L. Ryzhik, and K. Solna, 2004, Statistical stability in time reversal: SIAM J. Appl. Math., **64**, 1133–1155.

Rickett, J. and P. Sava, 2002, Offset and angle-domain common image-point gathers for shot-profile migration: Geophysics, **67**, 883–889.

Sava, P. and S. Fomel, 2003, Angle-domain common image gathers by wavefield continuation methods: Geophysics, **68**, 1065–1074.

———, 2006, Time-shift imaging condition in seismic migration: Geophysics, **71**, S209–S217.

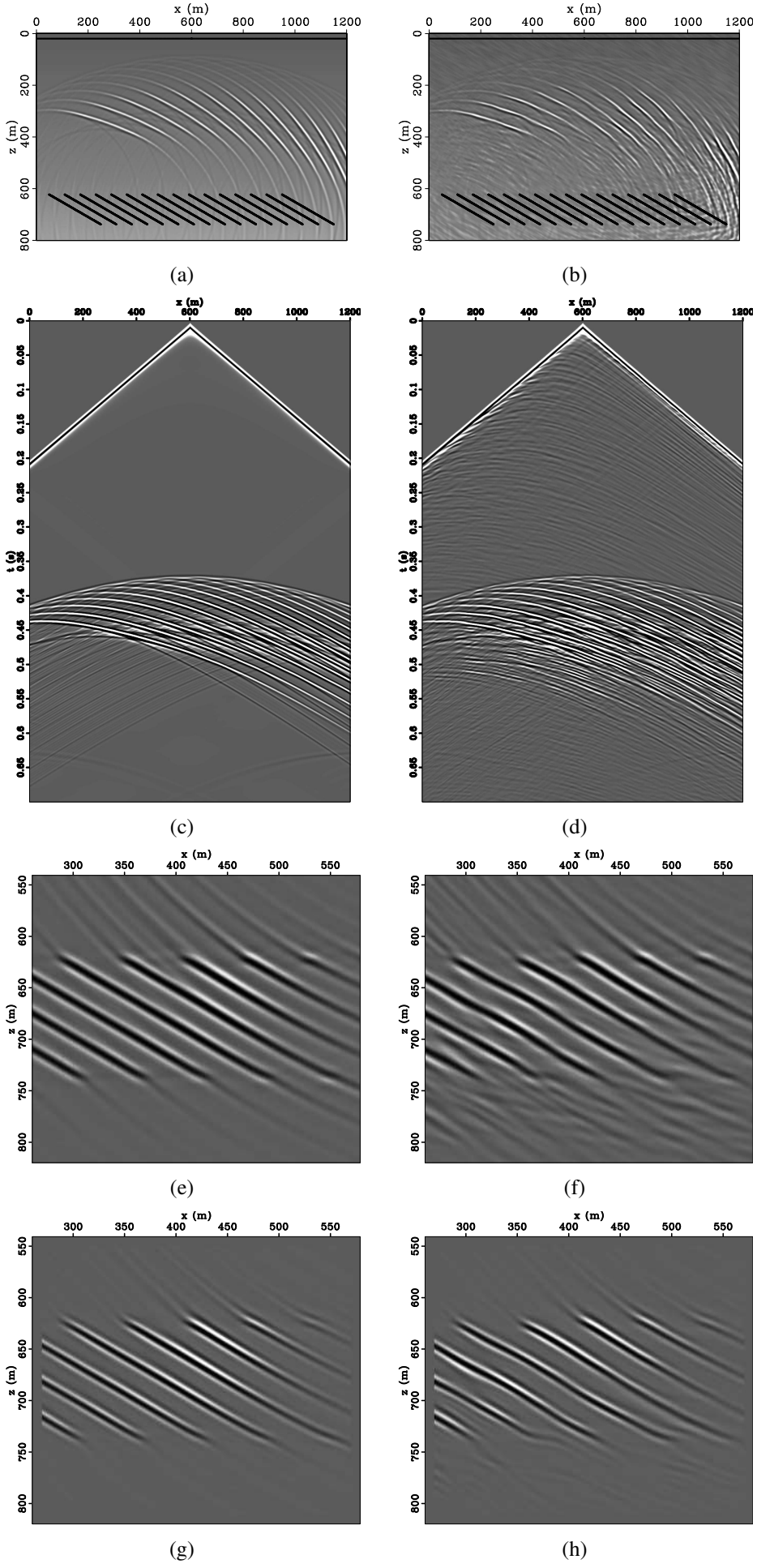


Figure 1: Velocity models and simulated wavefields (a)-(b), recorded data (c)-(d), migration with CIC (e)-(f), and with IIC (g)-(h).